



Cite this: *Chem. Commun.*, 2020, **56**, 8762

Received 2nd May 2020,
Accepted 29th June 2020

DOI: 10.1039/d0cc03163a

rsc.li/chemcomm

Enhancing the activity of photocatalytic hydrogen evolution from CdSe quantum dots with a polyoxovanadate cluster[†]

Emily H. Edwards,^{‡,a} Alex A. Fertig,^{‡,a} Kevin P. McClelland,^a Mahilet T. Meidenbauer,^a Saikat Chakraborty,^a Todd D. Krauss,^{ID *ab} Kara L. Bren^{ID *a} and Ellen M. Matson^{ID *a}

We report the improvement of photocatalytic proton reduction using molecular polyoxovanadate-alkoxide clusters as hole scavengers for CdSe quantum dots. The increased hydrogen production is explained by favorable charge interactions between reduced forms of the cluster and the charge on the quantum dots arising from the capping ligands.

Semiconducting nanocrystals, or quantum dots (QDs), have emerged as leading photocatalysts for visible light-driven charge-transfer reactions.^{1–4} Inspired by the creation of a solar fuel in natural photosynthesis, one of the most widely studied photocatalytic reactions using QDs is the reduction of protons to form hydrogen (H₂).^{5–7} When paired with sacrificial electron donors, cadmium selenide (CdSe) QDs are capable of photocatalytic proton reduction from the nanoparticle surface (*i.e.* without a co-catalyst).⁸ The yield of H₂ production can be significantly increased in the presence of a transition metal co-catalyst which facilitates charge separation⁹ and decreases the barrier for proton reduction.^{2,10–12} For example, in combination with a homogeneous nickel catalyst (“Ni-DHLA”; DHLA = dihydrolipoic acid), CdSe QDs produce H₂ with turnover numbers (TONs) up to 600 000 over two weeks in aqueous solution.¹³

Traditionally, research into the optimization of photocatalytic proton reduction with QDs has focused on improvements to the reduction co-catalyst. By comparison, less work has been dedicated to studying the subsequent charge balancing reactions that must occur through reduction of the QD. For

cadmium chalcogenides, the large effective mass of the hole relative to that of the electron makes hole transfer a likely rate-limiting step,^{3,14,15} limiting catalytic efficiency (Fig. 1). Some methods to improve hole-transfer rates have used modified ligands to delocalize the hole wave function.^{2,3,12,16} However, as a result of the chemical instability of these ligands,¹⁷ few studies have reported on their application in enhancing photocatalysis.^{18–20} Shelling the QD to form a type-II heterostructure is another viable method of separating the electron and hole, but this approach decreases catalytic efficiency by localizing one carrier to the core of the nanocrystal.²¹ Thus, a robust and efficient method of hole extraction from QDs remains necessary for improving photocatalytic systems.

A possible solution to enable efficient hole extraction is the coupling of QDs to either bulk or molecular metal oxides. Watson and coworkers have demonstrated that the mid-bandgap

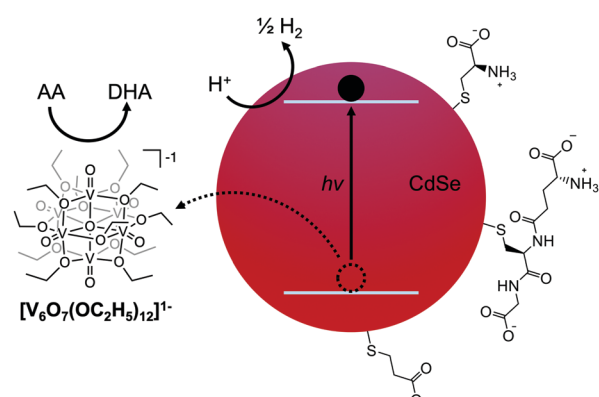


Fig. 1 Illustration of the general photocatalytic scheme. Upon excitation by visible light, the electron reduces protons at the surface of the QD, while the hole is extracted by a POV-alkoxide cluster. Ascorbic acid (AA) is used to regenerate the reduced form of the cluster in solution. Capping ligands were chosen to promote solubility in aqueous solutions, and include cysteine (top), glutathione (middle), and 3-mercaptopropionic acid (bottom). DHA indicates dehydroascorbic acid.

^a Department of Chemistry, University of Rochester, Rochester, New York 14627, USA. E-mail: krauss@chem.rochester.edu, bren@chem.rochester.edu, matson@chem.rochester.edu

^b The Institute of Optics, University of Rochester, Rochester, New York 14627, USA

† Electronic supplementary information (ESI) available: Experimental details, electronic absorption spectra, luminescence quenching analyses, cyclic voltammetry, hydrogen evolution curves, quantum yield calculations and tabulated results collected herein. See DOI: [10.1039/d0cc03163a](https://doi.org/10.1039/d0cc03163a)

‡ The authors contributed equally to this work.

states in doped V_2O_5 nanowires facilitate fast (<500 fs) hole transfer from CdSe QDs.²² The authors propose that the resulting charge-separated state could be used to delay charge recombination and improve photocatalytic proton reduction.^{22,23} In order to study homogeneous photocatalytic systems, we hypothesized that polyoxovanadate (POV) clusters could be used as an alternative to V_2O_5 nanowires for efficient hole extraction. While most POV clusters are isolated in their most-oxidized state (*i.e.* electron-deficient), the polyoxovanadate-alkoxide (POV-alkoxide) clusters explored in this study (Fig. 1) are reduced analogues of these metal oxide assemblies, rendering them well-suited to serve as hole-transfer reagents in photocatalytic schematics (Fig. S1, ESI[†]).²⁴ Indeed, POV-alkoxide clusters have been shown to reductively quench molecular chromophores for reactions such as water oxidation.²⁵ However, they have not been studied in combination with QD photosensitizers.

To test our hypothesis that charge transfer between photoexcited CdSe QDs and the POV-alkoxide cluster, $[\text{V}_6\text{O}_7(\text{OC}_2\text{H}_5)_{12}]^{1-}$, is possible, steady-state photoluminescence quenching experiments were conducted. Given previous activity of mid-sized CdSe QDs as photocatalysts, QDs with a first excitonic absorbance peak at 525 nm (± 5 nm) (correlating with a diameter of approximately 2.6 nm²⁶) capped with trioctylphosphine (TOP) ligands were synthesized (Fig. S2, ESI[†]).²⁷ Their luminescence was monitored in the presence of increasing equivalents of $[\text{V}_6\text{O}_7(\text{OC}_2\text{H}_5)_{12}]^{1-}$ (Fig. 2 inset). The photoluminescence of the QDs was efficiently quenched in the presence of the POV-alkoxide clusters, with a 96% decrease in emission intensity at 10 equivalents. The nonlinear behavior of the Stern–Volmer analysis suggests that the clusters quench the QD fluorescence through both static and dynamic mechanisms (Fig. S3, ESI[†]).²⁸ It is worth noting that there is a small overlap between the absorbance spectrum of $[\text{V}_6\text{O}_7(\text{OC}_2\text{H}_5)_{12}]^{1-}$ and the emission of CdSe QDs, so we cannot definitively rule out the possibility of

an energy transfer quenching mechanism (Fig. 2). However, given the low absorbance of the clusters at these concentrations, contributions from such a pathway are predicted to be negligible in comparison to those of charge transfer (Fig. S4; see ESI[†] for details).

Given the promising results from photoluminescence quenching (*vide supra*), we sought to probe the proton reduction characteristics upon the addition of $[\text{V}_6\text{O}_7(\text{OC}_2\text{H}_5)_{12}]^{1-}$ to a solution of glutathione-capped (CdSe –GSH) QDs and sacrificial electron donor ascorbic acid (Fig. 3). For this study, we opted to not include an external co-catalyst in an effort to simplify the already-complicated system, ensuring that any changes in catalysis were due to cluster/QD interactions. To establish a baseline for photoactivity of QDs under our conditions, a mixture of ascorbic acid and CdSe –GSH QDs, dissolved in ethanol and water (1:1), was irradiated with green ($530\text{ nm} \pm 10\text{ nm}$) light (Fig. 3 and Fig. S5, ESI[†]). Over 48 hours, the multicomponent system produces $110\text{ }\mu\text{mol} (\pm 42\text{ }\mu\text{mol})$ of H_2 . In the absence of ascorbic acid, negligible hydrogen evolution is observed (Fig. S6, ESI[†]). The rate of H_2 evolution remains constant over this time frame, indicating minimal degradation of the QDs, with an average rate of H_2 evolution of $2.22\text{ }\mu\text{mol h}^{-1} (\pm 0.78\text{ }\mu\text{mol h}^{-1})$. This correlates to a quantum yield (QY) of 8.0% ($\pm 2.4\%$) (see ESI[†] for details).

Upon addition of $[\text{V}_6\text{O}_7(\text{OC}_2\text{H}_5)_{12}]^{1-}$ ($100\text{ }\mu\text{M}$) to the photocatalytic system described above, both the average H_2 evolved in 48 hours and the rate of catalysis are approximately doubled (Fig. 3 and Fig. S5, ESI[†]). The total H_2 produced improves to $222\text{ }\mu\text{mol} (\pm 37\text{ }\mu\text{mol})$ with an improvement in rate to $4.61\text{ }\mu\text{mol h}^{-1} (\pm 0.85\text{ }\mu\text{mol h}^{-1})$, and an increase of 125% in average QY to 18% ($\pm 4.5\%$). To evaluate whether $[\text{V}_6\text{O}_7(\text{OC}_2\text{H}_5)_{12}]^{1-}$ might act as a H_2 -production catalyst, which would complicate its intended use as an electron mediator in this system, independent electrochemical analysis of the POV-alkoxide cluster was performed. Upon titration of 40 mM aqueous phosphate buffer ($\text{pH} = 6$) to a solution of 1 mM $[\text{V}_6\text{O}_7(\text{OC}_2\text{H}_5)_{12}]^{1-}$ and 0.1 M $[\text{Bu}_4\text{N}]^+\text{PF}_6^-$ in acetonitrile, no change in the electrochemical response of the cluster was observed, indicating that this reduced POV-alkoxide cluster is not active as a proton reduction catalyst (Fig. S7, ESI[†]). Taken together, these results support our hypothesis that POV-alkoxide clusters efficiently extract the hole from CdSe QDs, acting as a hole shuttle and resulting in improved production of H_2 .

Activity enhancement from the introduction of the POV-alkoxide cluster to the GSH-capped CdSe QDs prompted further exploration of the photocatalytic system. Given previously reported ligand-dependence on the photocatalytic activity of QDs,^{12,29–31} additional thiolate ligands were selected to determine if the mechanism of enhancement by $[\text{V}_6\text{O}_7(\text{OC}_2\text{H}_5)_{12}]^{1-}$ could be generalized to other QD-ligand systems. Cysteine (Cys) and 3-mercaptopropionic acid (MPA) were chosen as additional water-soluble ligands to cap QDs (Fig. 3A and Fig. S8, ESI[†]). The impact of the capping ligands on the first excitonic absorbance is small ($<10\text{ nm}$).

It has been previously reported that the degree of passivation of surface Cd^{2+} ions dramatically influences the yield of proton reduction for QDs in the absence of a co-catalyst.^{8,32,33}

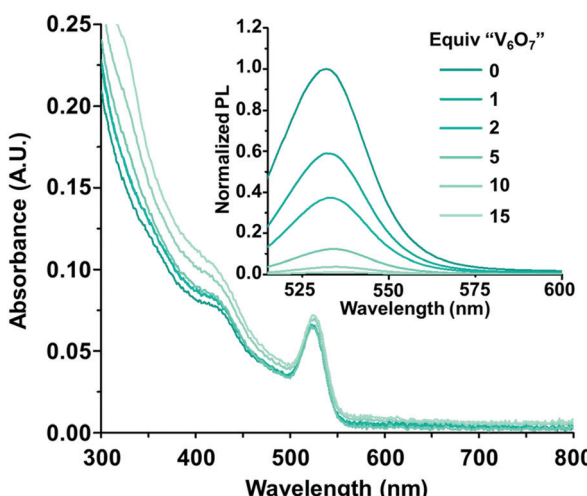


Fig. 2 The absorbance and photoluminescence (inset) spectra of CdSe –TOP with varying equivalents of $[\text{V}_6\text{O}_7(\text{OC}_2\text{H}_5)_{12}]^{1-}$ (" V_6O_7 "). All samples contained $1\text{ }\mu\text{M}$ CdSe with 0–15 equivalents of $[\text{V}_6\text{O}_7(\text{OC}_2\text{H}_5)_{12}]^{1-}$ in dichloromethane and the photoluminescence was normalized to the absorbance at the excitation wavelength (500 nm).

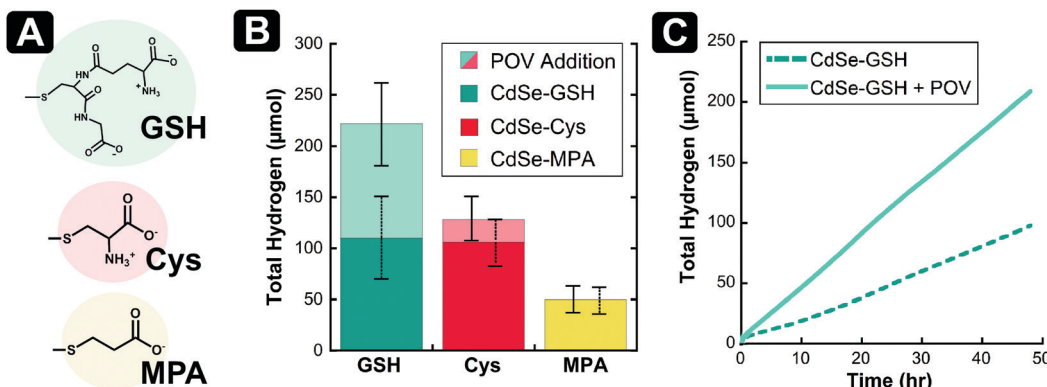


Fig. 3 (A) Structures of the capping ligands used on the surface of CdSe QDs; (B) total H₂ evolution after 48 hours from CdSe–GSH, CdSe–Cys, and CdSe–MPA in the presence of 0.5 M ascorbic acid, in a 1:1 EtOH : H₂O mixture, being irradiated by 530 nm light at 15 °C. Upon addition of 100 μM [V₆O₇(OC₂H₅)₁₂]¹⁻, the positive change in total H₂ production for CdSe–GSH and CdSe–Cys is shown (*n* = 3); (C) representative trials of H₂ evolution over time for the CdSe–GSH H₂ evolution system described in (B), showing improvement in the presence of [V₆O₇(OC₂H₅)₁₂]¹⁻.

Given the differences in the molecular structure of the three thiolate ligands investigated in this work, we anticipated that surface coverage would vary between GSH-, Cys- and MPA-capped QDs. Thus, to establish new baselines for H₂ production for each system, we evaluated the photocatalysis for the CdSe QDs in the absence of POV-alkoxide clusters. The CdSe–Cys and CdSe–MPA systems have slow H₂ evolution in the first ten hours of catalysis (Fig. S9 and S10, ESI†). After this induction period, H₂ generation is linear over the remainder of the experiment. This is in contrast to the GSH-capped QDs, which produce H₂ at a constant rate throughout the 48 hours of irradiation (Fig. 3C). In total, the Cys-capped CdSe QDs produce a similar amount of H₂ to those capped with glutathione ligands (106 μmol ± 22 μmol), while the CdSe–MPA analogues produce significantly less H₂ in the same time period (50 μmol ± 12 μmol) (Fig. S11, ESI†). Since proton reduction has been reported to occur at solvated Cd surface-sites,⁸ these differences in H₂ production without POV-alkoxide clusters suggest that MPA-capped QDs have a higher packing density than Cys- or GSH-capped QDs. This may be due to differences in the available binding modes of the ligands, or the ligand exchange procedures used.

Upon introduction of [V₆O₇(OC₂H₅)₁₂]¹⁻ to the photocatalytic experiments with Cys- and MPA-capped QDs, interesting trends were observed. As with GSH, Cys-capped CdSe QDs showed a boost in activity with the addition of POV-alkoxide clusters (Fig. 3 and Fig. S9, ESI†). In the presence of clusters, the average H₂ evolved increases to 128 μmol (±20 μmol) from 106 μmol (±22 μmol). In contrast, negligible change in the total production of H₂ is observed upon addition of POV-alkoxide cluster to the MPA-capped CdSe QDs (Fig. 3 and Fig. S10, ESI†; 50 μmol ± 12 μmol vs. 48 μmol ± 10 μmol with [V₆O₇(OC₂H₅)₁₂]¹⁻).

We justify the observed differences in H₂ production as resulting from differences in the interactions between the QDs and the POV-alkoxide clusters. The ligands chosen to probe the photocatalytic reactivity of these QDs have a different charge at pH = 4.5, thus providing a different surface chemistry for the photosensitizer. Glutathione is a zwitterionic tripeptide containing cysteine, glutamate, and glycine (*pK_as*: 2.1 (COOH),

3.5 (COOH), 8.8 (NH₃⁺)). It is anticipated that this ligand binds to the surface of the QD through the thiol moiety, allowing for the remaining charged regions of the ligand to interact with the environment.³⁴ At pH = 4.5, the amine group located on the GSH ligand will remain protonated (*i.e.* positively-charged) and may interact with the anionic charge-states of the POV-alkoxide cluster.³⁵ As charge transfer from the POV-alkoxide to the QD occurs, the anionic cluster cycles through higher oxidation states (*e.g.* [V₆O₇(OC₂H₅)₁₂]^{*n*}; *n* = 0, 1+, 2+), at which point the charge attraction with the amine group becomes less favorable. The diminished coulombic interaction between the anionic POV-alkoxide cluster and the positively charged residues at the QD surface drives more oxidized forms of the cluster away from the QD surface, preventing charge recombination *via* back electron transfer. The dissociated, oxidized form of the POV-alkoxide cluster subsequently reacts with ascorbic acid, resulting in re-reduction of the vanadium oxide assembly.

Supporting this mechanistic hypothesis, photocatalytic experiments with CdSe–Cys dots also showed an increase in the amount of H₂ produced in the presence of [V₆O₇(OC₂H₅)₁₂]¹⁻. Cysteine, an amino acid (*pK_as*: 1.8 (COOH), 10.7 (NH₃⁺)), has also been used as a zwitterionic capping ligand for QDs.^{12,36} The cysteine ligands offer a similar positively charged site for electrostatic interactions to occur, attracting the reduced cluster to the surface of the QD. We believe, however, that the smaller size of cysteine relative to glutathione leads to a more densely packed surface which inhibits the adsorption of [V₆O₇(OC₂H₅)₁₂]¹⁻, reducing the impact the clusters have on catalysis.

In contrast, CdSe–MPA showed no enhancement of H₂ production in the presence of [V₆O₇(OC₂H₅)₁₂]¹⁻. The absence of a positively charged residue in the MPA capping ligands would disfavor interaction between the QD and the reduced, anionic forms of the POV-alkoxide cluster. Instead, the more oxidized (cationic) states of the POV-alkoxide cluster (*e.g.* [V₆O₇(OC₂H₅)₁₂]^{*n*}; *n* = 1+, 2+) would be attracted to the QD surface. In these oxidation states, the cluster would energetically prefer to accept reducing equivalents from the QD, no longer functioning as a hole scavenging reagent. Also, as noted above, MPA-capped CdSe QDs appear

to have fewer uncoordinated sites, which could further inhibit interaction with the POV-alkoxide clusters and hole transfer from the QD.

Here, we have used POV-alkoxide clusters to efficiently extract photogenerated holes from CdSe QDs in order to significantly increase the volume of H₂ produced without the addition of a proton reduction co-catalyst. CdSe QDs capped with GSH show the largest increase in both the rate of reaction and the total amount of H₂ produced with the addition of POV-alkoxide clusters. Cys-capped QDs show a moderate increase in the amount of H₂ produced when clusters are present, while QDs capped with MPA show no significant increase in the amount of H₂ produced following addition of the vanadium oxide cluster. These results provide insight into the electrostatic interaction required for charge transfer between the photosensitizer and the cluster, which will aid in designing more efficient systems for the photocatalytic production of H₂.

This work is supported by the Chemical Sciences, Geosciences and Biosciences Division, Office of Basic Energy Sciences, Office of Science, U.S. Department of Energy, Grant No. DE-FG02-09ER16121. E. H. E. Acknowledges support from NIH training grant T32-GM118283.

Conflicts of interest

There are no conflicts to declare.

Notes and references

- 1 C. Huang, X.-B. Li, C.-H. Tung and L.-Z. Wu, *Chem. – Eur. J.*, 2018, **24**, 11530–11534.
- 2 M. S. Kodaimati, K. P. McClelland, C. He, S. Lian, Y. Jiang, Z. Zhang and E. A. Weiss, *Inorg. Chem.*, 2018, **57**, 3659–3670.
- 3 R. D. Harris, S. Bettis Homan, M. Kodaimati, C. He, A. B. Nepomnyashchii, N. K. Swenson, S. Lian, R. Calzada and E. A. Weiss, *Chem. Rev.*, 2016, **116**, 12865–12919.
- 4 D. J. Norris and M. G. Bawendi, *Phys. Rev. B: Condens. Matter Mater. Phys.*, 1996, **53**, 16338–16346.
- 5 J. Barber, *Chem. Soc. Rev.*, 2009, **38**, 185–196.
- 6 T. R. Cook, D. K. Dogutan, S. Y. Reece, Y. Surendranath, T. S. Teets and D. G. Nocera, *Chem. Rev.*, 2010, **110**, 6474–6502.
- 7 X.-B. Li, C.-H. Tung and L.-Z. Wu, *Nat. Rev. Chem.*, 2018, **2**, 160–173.
- 8 J. Zhao, M. A. Holmes and F. E. Osterloh, *ACS Nano*, 2013, **7**, 4316–4325.
- 9 V. V. Matylitsky, L. Dworak, V. V. Breus, T. Basché and J. Wachtveitl, *J. Am. Chem. Soc.*, 2009, **131**, 2424–2425.
- 10 F. F. Schweinberger, M. J. Berr, M. Döblinger, C. Wolff, K. E. Sanwald, A. S. Crampton, C. J. Ridge, F. Jäckel, J. Feldmann, M. Tschurl and U. Heiz, *J. Am. Chem. Soc.*, 2013, **135**, 13262–13265.
- 11 M. J. Berr, F. F. Schweinberger, M. Döblinger, K. E. Sanwald, C. Wolff, J. Breimeier, A. S. Crampton, C. J. Ridge, M. Tschurl, U. Heiz, F. Jäckel and J. Feldmann, *Nano Lett.*, 2012, **12**, 5903–5906.
- 12 E. A. Weiss, *ACS Energy Lett.*, 2017, **2**, 1005–1013.
- 13 Z. Han, F. Qiu, R. Eisenberg, P. L. Holland and T. D. Krauss, *Science*, 2012, **338**, 1321–1324.
- 14 K. E. Knowles, M. D. Peterson, M. R. McPhail and E. A. Weiss, *J. Phys. Chem. C*, 2013, **117**, 10229–10243.
- 15 P. V. Kamat, J. A. Christians and J. G. Radich, *Langmuir*, 2014, **30**, 5716–5725.
- 16 S. Lian, D. J. Weinberg, R. D. Harris, M. S. Kodaimati and E. A. Weiss, *ACS Nano*, 2016, **10**, 6372–6382.
- 17 R. D. Harris, V. A. Amin, B. Lau and E. A. Weiss, *ACS Nano*, 2016, **10**, 1395–1403.
- 18 J. R. Lee, W. Li, A. J. Cowan and F. Jäckel, *J. Phys. Chem. C*, 2017, **121**, 15160–15168.
- 19 O. M. Pearce, J. S. Duncan, N. H. Damrauer and G. Dukovic, *J. Phys. Chem. C*, 2018, **122**, 17559–17565.
- 20 C. M. Wolff, P. D. Frischmann, M. Schulze, B. J. Bohn, R. Wein, P. Livadas, M. T. Carlson, F. Jäckel, J. Feldmann, F. Würthner and J. K. Stolarecyk, *Nat. Energy*, 2018, **3**, 862–869.
- 21 T. X. Ding, J. H. Olshansky, S. R. Leone and A. P. Alivisatos, *J. Am. Chem. Soc.*, 2015, **137**, 2021–2029.
- 22 J. Cho, A. Sheng, N. Suwandaratne, L. Wangoh, J. L. Andrews, P. Zhang, L. F. J. Piper, D. F. Watson and S. Banerjee, *Acc. Chem. Res.*, 2019, **52**, 645–655.
- 23 J. L. Andrews, J. Cho, L. Wangoh, N. Suwandaratne, A. Sheng, S. Chauhan, K. Nieto, A. Mohr, K. J. Kadassery, M. R. Popeil, P. K. Thakur, M. Sfeir, D. C. Lacy, T.-L. Lee, P. Zhang, D. F. Watson, L. F. J. Piper and S. Banerjee, *J. Am. Chem. Soc.*, 2018, **140**, 17163–17174.
- 24 L. E. VanGelder, A. M. Kosswallaaraachchi, P. L. Forrestel, T. R. Cook and E. M. Matson, *Chem. Sci.*, 2018, **9**, 1692–1699.
- 25 M.-P. Santoni, G. La Ganga, V. Mollica Nardo, M. Natali, F. Puntoriero, F. Scandola and S. Campagna, *J. Am. Chem. Soc.*, 2014, **136**, 8189–8192.
- 26 W. W. Yu, L. Qu, W. Guo and X. Peng, *Chem. Mater.*, 2003, **15**, 2854–2860.
- 27 F. Qiu, Z. Han, J. J. Peterson, M. Y. Odoi, K. L. Sowers and T. D. Krauss, *Nano Lett.*, 2016, **16**, 5347–5352.
- 28 J. R. Lakowicz, in *Principles of Fluorescence Spectroscopy*, ed. J. R. Lakowicz, Springer, US, Boston, MA, 2006, pp. 277–330, DOI: 10.1007/978-0-387-46312-4_8.
- 29 A. Das, Z. Han, M. G. Haghghi and R. Eisenberg, *Proc. Natl. Acad. Sci. U. S. A.*, 2013, **110**, 16716–16723.
- 30 C. M. Chang, K. L. Orchard, B. C. M. Martindale and E. Reisner, *J. Mater. Chem. A*, 2016, **4**, 2856–2862.
- 31 M. Green, *J. Mater. Chem.*, 2010, **20**, 5797–5809.
- 32 M. J. Greaney, E. Couderc, J. Zhao, B. A. Nail, M. Mecklenburg, W. Thornbury, F. E. Osterloh, S. E. Bradforth and R. L. Brutchey, *Chem. Mater.*, 2015, **27**, 744–756.
- 33 W. D. Kim, J.-H. Kim, S. Lee, S. Lee, J. Y. Woo, K. Lee, W.-S. Chae, S. Jeong, W. K. Bae, J. A. McGuire, J. H. Moon, M. S. Jeong and D. C. Lee, *Chem. Mater.*, 2016, **28**, 962–968.
- 34 P. K. Sudeep, S. T. S. Joseph and K. G. Thomas, *J. Am. Chem. Soc.*, 2005, **127**, 6516–6517.
- 35 Z. Aliakbar Tehrani, Z. Jamshidi, M. Jebeli Javan and A. Fattahi, *J. Phys. Chem. A*, 2012, **116**, 4338–4347.
- 36 F. Shi, S. Liu and X. Su, *New J. Chem.*, 2017, **41**, 4138–4144.